Coordination and Supramolecular Chemistry of New Bis-bidentate Schiff-Base Ligands

Mauro Isola,*[a] Federica Balzano,[a] Vincenzo Liuzzo,[a] Fabio Marchetti,[a] Andrea Raffaelli,[b] and Gloria Uccello Barretta*[a]

The coordination chemistry of a series of bis-bidentate Schiff-base ligands with Ni^{II} and Cu^{II} has been investigated. The ligands contain two N,O-bidentate chelating salicylaldiminato units attached to polymethylene or α,α'-*ortho*-xylidene central spacers, through ether linkages at the 3-position of the salicyl moieties. In this paper we present a series of seven new complexes displaying several novel structural types, three of which are crystallographically characterized. Among others, the double-stranded helicates with the metal ions in the *trans*-square-planar geometry are of particular interest. The *ortho*-xylidene ligand H_2L^8, like the analogue H_2L^7 previously reported by us, forms dinuclear double-stranded helicates stable both in the solid state and in solution; in the case of the ligands $H_2L^{1–6}$, the nuclearity and the structural motif of the related complexes depend on the number (n) of methylene units in the bridge. When $n = 3, 4$, thermodynamically stable products from their reaction with Ni^{II} and Cu^{II} are oligomeric or polymeric species, while under kinetic control novel supramolecular architectures become accessible. The Ni^{II} complexes of the ligands with $n = 5, 6, 8$ exist as dinuclear double-stranded helicates in the solid state, while in solution they exhibit a monomer–dimer interconversion process, which has been studied using Diffusion Ordered Spectroscopy (DOSY).

(© Wiley-VCH Verlag GmbH & Co. KGaA, 69451 Weinheim, Germany, 2008)

Introduction

The assembly of architecturally sophisticated, high-nuclearity coordination complexes from the reactions of relatively simple ligands with suitable metal ions has been receiving considerable attention.[1] Indeed, the development of simple synthetic procedures for the preparation of new systems from relatively inexpensive starting materials is one of the major goals in the field of metallosupramolecular chemistry. In this context, a number of attractive ligands have been reported which contain two bidentate chelating arms linked by a central flexible bridge. Most examples of this type of ligand present all nitrogen donor sets, but recently numerous examples of O,O and N,O mixed-donor ligands have been described.[2]
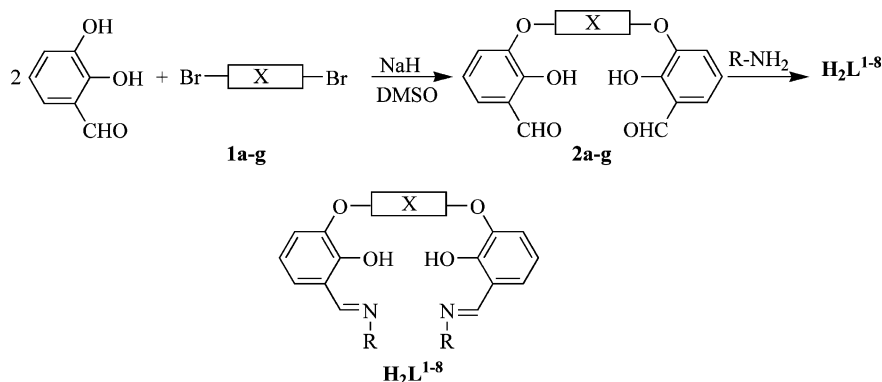
We have previously reported a simple synthetic method for the construction of nickel(II)-assisted supramolecular structures of bis-N,O-bidentate Schiff bases using commercially available starting materials.[3] These Schiff-base ligands contain two salicylaldiminato units connected by an α,ω-dioxo-polymethylene or by the α,α'-dioxo-xylidene spacer through the 3-position of salicyl moieties (Scheme 1). In these studies, we showed that the ligand H_2L^2 forms a trinuclear circular helicate, while the H_2L^5 and H_2L^7 ligands yield double-helical dinuclear complexes based on a square-planar geometry, an unusual coordination geometry around the metal centres of these supramolecular motifs. Furthermore, as a remarkable difference in the behaviour of the dinuclear helicate of H_2L^5 and H_2L^7, a dinuclear/mononuclear equilibrium was observed in $CHCl_3$ solutions of the first complex, while the second one is stable both in solid state and in solution.

The approach that we explore herein is to modify the length and flexibility of the bridge of this class of ligands with the goal of influencing the nuclearity and the architecture of their complexes. Thus, in this paper we report the synthesis and characterization of new members of our family of ligands (H_2L^1, H_2L^3, H_2L^4 and H_2L^8) and their Ni^{II} complexes, the complexation studies of H_2L^1 and H_2L^8 with Cu^{II}, as well as NMR investigations on the reversible interconversion between the mononuclear species and dinuclear helicates of the Ni^{II} complexes of H_2L^3 and H_2L^4.

[a] Dipartimento di Chimica e Chimica Industriale, Università di Pisa,
Via Risorgimento 35, 56126 Pisa, Italy
Fax: +39-050-2219260
E-mail: misola@dcci.unipi.it
gub@dcci.unipi.it
[b] Istituto di Chimica dei Composti Organo-Metallici – Sezione di Pisa, Dipartimento di Chimica e Chimica Industriale, Università di Pisa,
Via Risorgimento 35, 56126 Pisa, Italy

Scheme 1 structures (1a-g, 2a-g, H₂L¹⁻⁸)

X	Dibromide	R	Ligand	Complexes
$-(CH_2)_3-$	1a	nPr	H_2L^1	$[Ni_2(L^1)_2]$,[a] $[Ni_x(L^1)_x]$[a] $[Cu_2(L^1)_2]$,[a] $[Cu_x(L^1)_x]$[a]
$-(CH_2)_4-$	1b	nPr	H_2L^2	$[Ni_x(L^2)_x]$,[b] $[Ni_3(L^2)_3(py)_6]$[b] $[Ni_3(L^2)_2(CH_3CO_2)_2]\cdot CH_3CN$[a]
$-(CH_2)_5-$	1c	nPr	H_2L^3	$[NiL^3]$,[a] $[Ni_2(L^3)_2]$[a]
$-(CH_2)_6-$	1d	nPr	H_2L^4	$[NiL^4]$,[a] $[Ni_2(L^4)_2]$[a]
$-(CH_2)_8-$	1e	nPr	H_2L^5	$[NiL^5]$,[b] $[Ni_2(L^5)_2]\cdot THF$[b]
$-(CH_2)_{12}-$	1f	nPr	H_2L^6	$[NiL^6]$[b]
(o-xylylene)	1g	Me	H_2L^7	$[Ni_2(L^7)_2]\cdot CHCl_3$,[c] $[Cu_2(L^7)_2]$[c]
		nPr	H_2L^8	$[Ni_2(L^8)_2]$,[a] $[Cu_2(L^8)_2]$[a]

[a] This work. [b] Ref.[3a]. [c] Ref.[3b]

Scheme 1. Synthesis of the ligands and related Ni^{II} and Cu^{II} complexes.

Results and Discussion

The new ligands H_2L^1, H_2L^3, H_2L^4 and H_2L^8 were easily prepared in good overall yields (50–60%) following the general procedure previously described[3] for the other ligands presented in Scheme 1.

The dianion of 2,3-dihydroxybenzaldehyde was generated by reaction with NaH in DMSO.[4] Subsequent nucleophilic displacement of the bromides from the appropriate dibromides 1a–g yielded dialdehydes 2a–g. The ligands were prepared by imine condensation of the dialdehydes with the appropriate amine. Clearly, this methodology is suitable for the preparation of a range of bis-chelating ligands with two salicylaldimine units by varying the structural parameters of the spacers (length and flexibility) and the substituents on the imine nitrogen atoms. All of the ligands gave correct elemental analyses and were further characterized by IR and ^{1}H NMR spectroscopy (see NMR section).

Ni^{II} and Cu^{II} Complexes of H_2L^1

The reaction of equimolar amounts of [Ni(OAc)$_2$]·4H$_2$O or [Cu(OAc)$_2$]·4H$_2$O with H_2L^1 in ethanol at room temperature rapidly afforded light-green or light-brown solids, respectively, partly soluble in chloroform or dichloromethane. The chloroform solutions of these solids upon addition of CH$_3$CN gave materials practically insoluble in the same solvents where they were initially soluble. Elemental analyses of the soluble and insoluble batches supported the formation of metal/ligand 1:1 complexes. Furthermore, the IR

spectra of all the batches are very similar and display a strong absorption characteristic of the C=N bond (at 1614 and 1616 cm^{-1} for the Ni^{II} and Cu^{II} derivatives, respectively) shifted to lower frequency relative to that of the free ligand (1635 cm^{-1}), clearly indicative of metal complexation. ESI-MS spectra of CHCl$_3$–CH$_3$CN solutions display major peaks (with the correct isotopic distributions) corresponding to $[Ni_2(L^1)_2+Na]^+$ (m/z 934), $[Cu_2(L^1)_2+H]^+$ (m/z 921) and $[Cu_2(L^1)_2+Na]^+$ (m/z 944), evidently indicating the presence of a dinuclear structure in solutions for both derivatives, namely $[Ni_2(L^1)_2]$ and $[Cu_2(L^1)_2]$.

The nickel derivative, in both the soluble and insoluble forms, is diamagnetic, suggesting a square-planar geometry around the Ni^{II} ions. Furthermore, its ^{1}H NMR spectrum in CDCl$_3$ is relatively simple and shows a single set of signals that can be fully assigned, which suggests that it exists as a single species in solution. Unfortunately, we were not able to obtain crystals suitable for X-ray diffraction, so we cannot infer the spatial arrangement of the NiN$_2$O$_2$ coordination planes for this dinuclear complex in the solid state. In solution, the ^{1}H NMR spectroscopic data do not support a helical array (see NMR studies on the double-stranded helicates); in fact, in comparison with the free ligand, the complex has only modest up-field shifts for most protons, the largest being $\Delta\delta \approx 0.3$ ppm. On the contrary, in the case of the double-stranded helicate $[Ni_2(L^7)_2]$ methylene protons are diastereotopic and the resonances of the imine and N-methyl groups undergo remarkable changes ($\Delta\delta \approx 1.5$ and 1.2 ppm, respectively) upon coordination, as

the helical arrangement constrains these protons in the shielding region generated by the aromatic rings.[3b] In the present case, where the short trimethylene spacer is expected to induce steric disposal not very dissimilar to that generated by the *ortho*-xylidene bridging unit of $[Ni_2(L^7)_2]$, the ^{1}H NMR spectroscopic data seem consistent with the adoption of a more symmetrical nonhelical face-to-face structure, which can accommodate the short bridge more easily than the helical one. Figure 1 (a) shows the schematic representation of this presumed structure of $[Ni_2(L^1)_2]$, where the nickel atoms are linked in the *trans*-square-planar geometry (the *cis* geometry is prevented from steric crowding of the N-substituents), the phenyl rings and the chelating arms from one ligand are superimposed, and the imine protons as well as those of the N-substituents are protruding outside the coordination planes, far from the shielding cone of the aromatic rings.
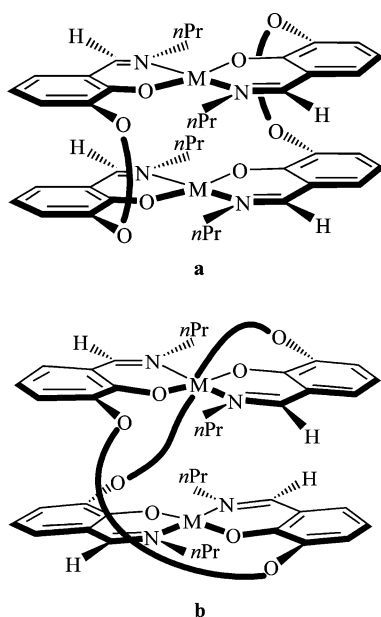

Figure 1. Schematic representations of dinuclear face-to-face (a) and double-stranded helical (b) structure of the Ni[II] and Cu[II] complexes; the metal ions exhibit a square-planar geometry. The curves represent polymethylene or *o*-xylidene bridges. The coordination planes can rotate around the M···M axes depending on the length of the bridges.

For the dinuclear complex $[Cu_2(L^1)_2]$, the lack of experimental (NMR and magnetic) data and the coordination plasticity of the Cu[II] ion, which may provide access to a variety of coordination geometries, do not allow any reasonable hypothesis on its structure. Nevertheless, the analogy found between $[Ni_2(L^7)_2]$ and $[Cu_2(L^8)_2]$ (vide infra) suggests the square-planar coordination geometry and the face-to face structure as a possible spatial disposition also for this complex.

Concerning the observed conversion of the initially formed soluble derivatives of both Ni[II] and Cu[II] to insoluble and intractable materials, it is very likely that it is a process of rearrangement of kinetic products, namely the dinuclear complexes $[Ni_2(L^1)_2]$ and $[Cu_2(L^1)_2]$, to oligo-

meric or polymeric species – where the ligand structure and the salicylaldiminato nature of the complexes remain unmodified, as suggested by the IR data – thermodynamically favoured by the absence of steric constraints.

Ni[II] Complexes of H_2L^2

In a previous communication[3a] we reported that the reaction of H_2L^2 with nickel(II) acetate resulted in the formation of a 1:1 oligomeric or polymeric material, insoluble in common organic solvents. However, this material was soluble in pyridine and from the pyridine solution the paramagnetic complex of stoichiometry $[Ni_3(L^2)_3(py)_6]$ was precipitated upon addition of Et₂O. The X-ray crystal structure of this compound revealed the complex to be a trimer and possess a trinuclear circular helical architecture, a relatively rare class of compounds.[1c,5] This is recalled in Figure S1 (see Supporting Information), which illustrates the octahedral coordination geometry of each nickel(II) ion (two pairs of O,N coordination sites of two different ligands and two pyridine nitrogen atoms) and its helical nature.

It is now fairly well established that assembly processes involving polynucleating and flexible ligands are expected to be dependent on the reaction conditions, especially reagent concentrations.[5a,5e,6] Consequently, our next step was to investigate the effect of conducting the reaction at higher dilution to reduce intermolecular complexation that favours the polymer formation. In fact, slow addition of a nickel acetate solution in methanol (9.7 mM) to a 1.6 mM solution of H_2L^2 in methanol, at room temperature, yielded a microcrystalline green solid, soluble in CHCl₃, CH₂Cl₂, MeOH and CH₃CN. ESI-MS data indicated a 3:2 metal:ligand ratio and the presence of two acetate ions with the peak at highest m/z being 1133, which corresponds to $[Ni_3(L^2)_2 \cdot (OAc)_2 + Na]^+$. Slow evaporation of a solution of the complex in CH₃CN afforded X-ray-quality crystals: the structure of the compound is shown in Figure 2. The complex has the formulation $[Ni_3(L^2)_2 \cdot (OAc)_2] \cdot CH_3CN$ and is a dimer that possesses a wrinkled metallomacrocyclic structure with a molecule of nickel acetate coordinated in its cavity. The two bridging ligands adopt significantly different conformations and denticities: one ligand (yellow in part B of Figure 2) coordinates, as usual, each *N,O*-bidentate arm to a different metal centre, while the other, $(L^2)^{2-}$, acts as a hexadentate chelate ligand capable of coordinating both ethereal oxygen atoms in addition to the *N,O*-bidentate moieties. Each metal ion has a distorted octahedral geometry and the distortion amount may be inferred from the bond lengths listed in Table 1 and from the remark that the L–Ni–L angles, where L means O or N, range between 75.6° and 173.6° for Ni(1), between 75.7° and 176.4° for Ni(2) and between 75.4° and 175.1° for Ni(3). The nickel atoms which are part of the macrocyclic skeleton are linked by two *N,O*-coordination sites of different ligands and one oxygen atom from each acetate ion, while the encapsulated Ni[II] reaches the hexacoordination by bonding four oxygen atoms (two ethereal and two phenolic) from the hexadentate ligand and two oxygen atoms from the acetate ions,

which act as bidentate ligands. The phenyl rings, with the adjacent chelating groups, lie two below (N and P in part B of Figure 2; centroid–centroid 8.89 Å) and two above (M and Q in Figure 2, B; centroid–centroid 8.96 Å) the plane of the metal centres.
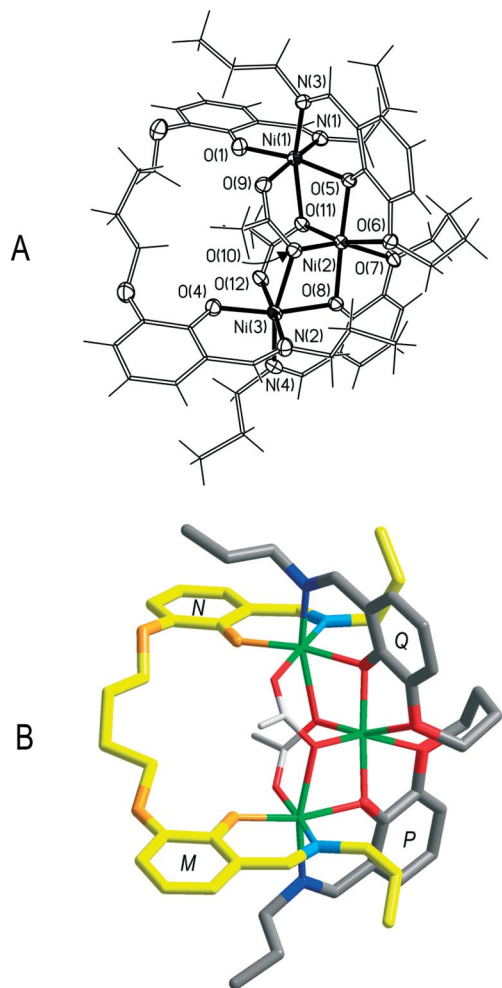

Figure 2. Molecular structure of the complex [Ni$_3$(L^2)$_2$·(OAc)$_2$]. (A) View illustrating the distorted octahedral geometry of the metal. (B) Stick representation; the Schiff ligands are distinguished by colour, emphasizing the cavity with the encapsuled Ni^{II} and acetate ions (lines).

Table 1. Bond lengths [Å] around the Ni atoms in [Ni$_3$(L^2)$_2$·(OAc)$_2$].

Ni(1)–O(1)	1.954(3)	Ni(2)–O(8)	1.986(2)
Ni(1)–O(5)	2.023(3)	Ni(2)–O(10)	1.997(3)
Ni(1)–N(1)	2.051(3)	Ni(2)–O(11)	2.003(3)
Ni(1)–N(3)	2.059(3)	Ni(3)–O(4)	1.974(3)
Ni(1)–O(9)	2.098(3)	Ni(3)–O(8)	2.035(2)
Ni(1)–O(11)	2.348(3)	Ni(3)–N(2)	2.052(3)
Ni(2)–O(5)	1.990(2)	Ni(3)–N(4)	2.068(3)
Ni(2)–O(6)	2.149(3)	Ni(3)–O(10)	2.296(3)
Ni(2)–O(7)	2.226(3)	Ni(3)–O(12)	2.091(3)

It is noteworthy that this supramolecular structure is also very stable in solution, as demonstrated by the presence of the molecular peak in the ESI-MS spectrum and the observation that it can be recovered unmodified from solutions in polar and protic solvents.

Ni^{II} Complexes of H$_2$L^3 and H$_2$L^4

Interestingly, we found[3a] that the ligand with the octa-methylene spacer, H$_2$L^5, affords the double-helical dinuclear complex [Ni$_2$(L^5)$_2$]·THF by a self-assembly process, where each nickel atom is linked in a *trans*-square-planar geometry, the first example of helicate based on this coordination geometry. However, this complex in CHCl$_3$ solution undergoes a disassembly process which results in an equilibrium mixture of mono- and dinuclear species. These results prompted us to study the coordination chemistry of ligands that have a number of methylene spacers intermediate between four and eight and the properties of their Ni^{II} complexes. Thus, the ligands H$_2$L^3 and H$_2$L^4 were easily prepared by using the same general method as used for the other ligands, and their coordination to nickel(II) was achieved by stirring 1 equiv. of nickel(II) acetate with 1 equiv. of the ligand in ethanol. In both cases green precipitates were formed, which were isolated by filtration. The ESI mass spectra show peaks corresponding to [Ni$_2$(L^3)$_2$+H$^+$] (*m/z* 965), [NiL^3+H$^+$] (*m/z* 483), [Ni$_2$(L^4)$_2$+H$^+$] (*m/z* 993) and [Ni(L^4)+H$^+$] (*m/z* 497). These data are consistent with the coexistence in solution of a dinuclear and mononuclear species in both cases, as has been confirmed by ^{1}H NMR studies (vide infra).

Green crystals of [Ni$_2$(L^3)$_2$]·*n*-heptane were obtained by slow evaporation of saturated chloroform/*n*-heptane solutions of the corresponding complexes (Table 2). The X-ray structural analyses clearly show (Figure 3; a stick-and-ball representation is presented in Figure S2 in the Supporting Information) that the compound has a dinuclear helical structure with the nickel(II) centres in a *trans*-square-planar geometry, linked by *N,O* coordination sites from two different ligands, the same as in [Ni$_2$(L^5)$_2$]·THF (and in [Ni$_2$(L^7)$_2$]·CHCl$_3$ and [Cu$_2$(L^8)$_2$], vide infra).

Table 2. Bond lengths [Å] and angles [°] around the Ni atom in [Ni$_2$(L^3)$_2$].

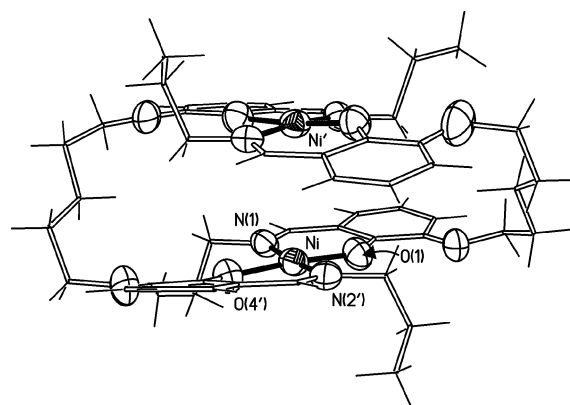| Ni–O(1)	1.817(7)	Ni–N(1)	1.876(10)
Ni–O(4')	1.829(7)	Ni–N(2')	1.905(10)
O(1)–Ni–N(1)	93.1(4)	O(1)–Ni–N(2')	86.7(4)
O(4')–Ni–N(2')	93.4(4)	O(4')–Ni–N(1)	87.2(4)
O(1)–Ni–O(4')	175.4(3)	N(1)–Ni–N(2')	175.7(3)

Figure 3. Molecular structure of the complex [Ni$_2$(L^3)$_2$] projected in a direction near to the twofold axis. Thermal ellipsoids of Ni, N and O atoms are at 30% probability; ' denotes *y, x, –z*.

The molecule shows a C_2 symmetry; the twofold axis passes between the Ni atoms in a direction approximately perpendicular to the projection plane of Figure 3. Although the coordination around the metals is almost perfectly planar (max. deviations 0.07 Å), the limited length of the ligand causes the salicylaldiminate moieties to bend, making moderately bowed surfaces towards the interior of the molecule with a phenyl(centroid)–Ni–phenyl(centroid) angle of 173.9° and a Ni···Ni′ distance of 3.617 Å. If we consider fully eclipsed (rotation angle 0°) two metal coordination squares where the M–N and M–O bonds (M = Ni, Cu) of a coordination plane eclipse, respectively, the M–O and M–N bonds of the other plane, as in Figure 1 (b), the coordination squares in $Ni_2(L^3)_2$ are staggered by a rotation of about 29.5°. In comparison to the complex $[Ni_2(L^5)_2]\cdot THF$, containing the long octamethylene bridge, the coordination environments around the metal centres of the complex $[Ni_2(L^3)_2]$ show a similar deviation from the planarity (max. deviations 0.31 Å vs. 0.22–0.31 Å) but a significantly higher rotation value around the Ni···Ni axis (angle of about 29.5° vs. 3.5°), evidently as a consequence of the constraints introduced by the shorter pentamethylene bridge.

For the complex $[Ni_2(L^4)_2]$ we were not able to obtain crystals suitable for X-ray diffraction analysis. However, owing to the bridge length of H_2L^4 intermediate between those of H_2L^3 and H_2L^5, the presence of a helical arrangement is both unambiguous and consistent with ^1H NMR studies in solution (see NMR section).

Cu^{II} and Ni^{II} Complexes of H_2L^8

The ligand H_2L^8, which possesses a skeleton identical to that of ligand H_2L^7 but with the N-n-propyl instead of the N-methyl group, was introduced to prepare more soluble complexes and to confirm the ability of the rigid ortho-xylidene bridge to favour the self-assembly of stable double helicates.

The reaction of Ni^{II} and Cu^{II} acetates with ligand H_2L^8, performed under the usual conditions, led to the assembly of the dinuclear complexes $[Ni_2(L^8)_2]$ and $[Cu_2(L^8)_2]$ as green and brown microcrystalline solids, respectively. Elemental analyses show the correct composition for the compounds, and characteristic peaks are observed in the ESI mass spectra for the dinuclear complexes. Furthermore, according to NMR measurements performed on $[Ni_2(L^7)_2]\cdot CHCl_3$ and $[Ni_2(L^8)_2]$ (see NMR section and ref.[3b]), MS/MS experiments have suggested that the dinuclear complexes are the unique molecular species in solution; in fact, these experiments showed that the important ions observed in the spectra of $[Ni_2(L^8)_2]$ and $[Cu_2(L^8)_2]$ arise from the fragmentation of the main peaks at m/z = 1033 and 1046, respectively.

Single brown crystals of $[Cu_2(L^8)_2]$ were obtained by slow crystallization from chloroform/n-heptane solutions. The molecular structure (Figure 4; a stick-and-ball representation is presented in Figure S3 in the Supporting Information) shows the complex to be a double helicate with C_2

symmetry similar to that of $[Ni_2(L^7)_2]\cdot CHCl_3$ (pseudo-C_2) and $[Ni_2(L^3)_2]$, but different from them in that the twofold axis is parallel to the coordination planes; in $[Cu_2(L^8)_2]$ the twofold axis crosses the copper atoms. The geometry of the bonding around Cu is described in Table 3. The Cu-salicyl-aldiminato moieties make surfaces with a more pronounced curvature with respect to the nickel derivatives, as evidenced by the closer angles between the centroids of the salicyl rings and the metal centres {153.7° and 164.4° vs. 173.9° of $[Ni_2(L^3)_2]$ and 175.0° of $[Ni_2(L^7)_2]\cdot CHCl_3$} and by the longer Cu···Cu distance (3.784 Å) compared to the Ni···Ni distances in $[Ni_2(L^7)_2]\cdot CHCl_3$ and $[Ni_2(L^3)_2]$ (3.554 Å and 3.617 Å, respectively). Each phenylene ring of the bridge is approximately perpendicular only to one of the adjacent salicyl rings (angle of 89.3°), while with the other one it makes a smaller angle (67.1°); these differences probably reflect the large distortion from the trans-planar coordination around the copper centres, owing to their coordination plasticity. The coordination squares are rotated with respect to each other around the Cu···Cu axis with an angle of ca. 42°, similar to that found in $[Ni_2(L^7)_2]\cdot CHCl_3$ around the Ni···Ni axis (43.7°).
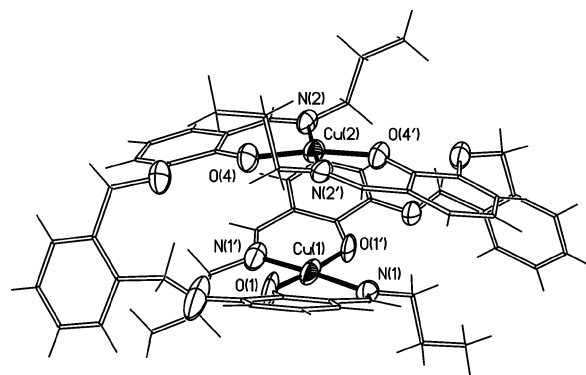

Figure 4. Molecular structure of the helical complex $[Cu_2(L^8)_2]$. Thermal ellipsoids of Cu, N and O atoms are at 30% probability; ′ denotes –x, y, 1/2 – z.

Table 3. Bond lengths [Å] and angles [°] around Cu atoms in $[Cu_2(L^8)_2]$.

Cu(1)–O(1)	1.917(12)	Cu(1)–N(1)	1.989(11)
Cu(2)–O(4)	1.886(5)	Cu(2)–N(2)	1.978(7)
O(1)–Cu(1)–N(1)	92.7(5)	O(1)–Cu(1)–N(1′)	87.5(5)
O(1)–Cu(1)–O(1′)	173.6(6)	N(1)–Cu(1)–N(1′)	176.7(7)
O(4)–Cu(2)–N(2)	91.5(3)	O(4)–Cu(2)–N(2′)	89.4(3)
O(4)–Cu(2)–O(4′)	169.7(4)	N(2)–Cu(2)–N(2′)	170.3(5)

Unfortunately the crystalline solid of $[Ni_2(L^8)_2]$ was not suitable for X-ray diffraction, so the double helical nature of this complex can only be demonstrated in solution (see next paragraph), but there is no doubt that, considering the essentially identical structures of the ligands H_2L^7 and H_2L^8, very close analogies must exist in the structural features of the solid state of their nickel complexes. On the basis of these considerations, unambiguous proof of the previously[3b] proposed helicate structure of $[Cu_2(L^7)_2]$ came from the crystal structure of $[Cu_2(L^8)_2]$.

NMR Studies on the Stability of the Double Helicates in Solution

Interconversion processes between complexes with different nuclearity, involving helicates or other supramolecular structures, have been reported to be operating in several systems.[7] In certain cases these processes are achieved by adding an external cation[7b,7j] or anion[7a] that, through host–guest interactions, promotes the conversion of a structure to a larger one where it remains encapsulated. Alternatively, as described by Lehn and co-workers in a recent interesting paper,[7g] the addition of Ag+ ions prompts the conversion of polyheterocyclic monostranded helical ligands to dinuclear double-stranded helicates; the reversibility of the process is implemented by the addition of a strong cryptand which scavenges Ag+ and releases it by protonation. In another recent paper,[7c] Lehn and co-workers studied the reversible assembly of helical monostranded oligopyridine into double-helical dimers as a result of a balance among multiple competing interactions (intra- and intermolecular hydrogen bonding, extensive intermolecular aromatic stacking stabilizing the double-stranded helices).

As reported before, the dinuclear helicate $[Ni_2(L^5)_2]\cdot THF$ undergoes a disassembly process on dissolution in chloroform, without intervention of other species.[3a] This process appears to be the result of the predominance of the solvation energy of the mononuclear complex and of the absence of strong noncovalent CH–π and π–π interactions which might contribute to the stabilisation of the dinuclear helicate. The flexibility of the octamethylene bridging unit presumably confers geometrical requirements on the ligand framework to favour the disassembling action of the solvent and the formation of a stable mononuclear species. According to this interpretation, replacement of the octamethylene with the rigid *ortho*-xylidene unit resulted in the formation of the double-stranded helicate $[Ni_2(L^7)_2]\cdot CHCl_3$, stable in chloroform solution.[3b] In light of these results, we envisaged that helicates derived from ligands with intermediate bridge length and flexibility, such as $[Ni_2(L^3)_2]$ and $[Ni_2(L^4)_2]$, should exhibit an intermediate behaviour.

The nickel complexes $[Ni_2(L^3)_2]$, $[Ni_2(L^4)_2]$ and $[Ni_2(L^8)_2]$ were characterized by NMR spectroscopy by analyzing homonuclear and heteronuclear scalar and dipolar interactions in the Double Quantum Filtered-Correlation Spectroscopy (DQF-COSY), Rotating-Frame Overhauser Enhancement Spectroscopy (ROESY) and gradient Heteronuclear Single Quantum Coherence (gHSQC) maps.

The numbering scheme employed for the ^{1}H NMR characterization of nickel complexes is reported in Scheme 2.

Information on the molecular sizes of the complexes to be correlated to their nuclearities were obtained by Diffusion-Ordered Spectroscopy (DOSY) measurements in solution.[8] The DOSY technique makes it possible to measure diffusion coefficients (*D*) in solution, which, for spherical species, can be correlated to the hydrodynamic radius R_H by means of the Stokes–Einstein equation [Equation (1)] where *k* is the Boltzmann constant, *T* is the temperature and *η* is the viscosity of the solvent:

$$D = \frac{kT}{6\pi\eta R_H}$$

(1)

Therefore diffusion coefficients represent global parameters, which are characteristic of molecular species as a whole. In this respect these parameters have great potentialities in the detection of complexed species, where an increase of molecular sizes, and hence a decrease of diffusion coefficients with respect to uncomplexed forms, should be expected.
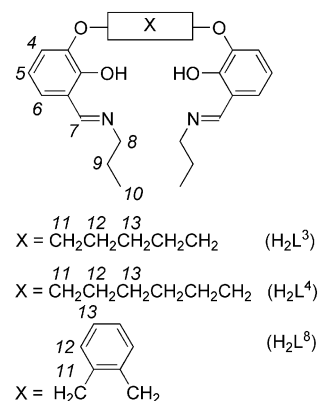
Scheme 2. Numbering scheme employed for the ^{1}H NMR characterization of nickel complexes.

The $[Ni_2(L^3)_2]$ complex can be usefully employed as the basis for our discussion, as its behaviour in solution, as detected by NMR spectroscopy, gathers together several common features of this kind of complex: in the freshly prepared samples a pure dinuclear species was detected, which, in time, undergoes disassembly towards species, the nature of which will be discussed.

The ^{1}H NMR spectrum (Figure 5, a) of a freshly dissolved sample in CDCl₃ solution showed only the expected set of resonances for each proton or group of equivalent protons (Table 4). Among assigned resonances, a surprisingly high anisochrony was detected for the methylene protons H-8 directly bound to the imine nitrogen, which originated two resonances at δ = 4.16 ppm and 1.32 ppm
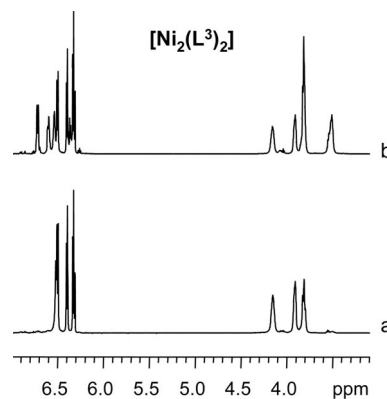

Figure 5. ^{1}H NMR (600 MHz, CDCl₃, 25 °C) spectral region (3.0–7.0 ppm) of $[Ni_2(L^3)_2]$ freshly dissolved (a) and one week after dissolution (b).

Table 4. ^{1}H NMR (300 MHz, CDCl$_3$, 25 °C) chemical shift (δ in ppm referenced to TMS as external standard) data of ligands H$_2$L^3 and H$_2$L^4, dinuclear [Ni$_2$(L^3)$_2$] and [Ni$_2$(L^4)$_2$] complexes, and mononuclear [NiL^3] and [NiL^4] complexes.

Proton	H$_2$L^3	Dinuclear [Ni$_2$(L^3)$_2$]		Mononuclear [NiL^3]	
	δ	δ	m[a] (J, Hz)	δ	m[a] (J, Hz)
4	6.90	6.51	d (J = 7.8)	6.61	d (J = 7.8)
5	6.75	6.33	dd (J = 7.8, J = 7.8)	6.37	dd (J = 7.8, J = 7.8)
6	6.85	6.41	d (J = 7.8)	6.73	d (J = 7.8)
7	8.30	6.49	br. s	7.92	br. s
8	3.55	4.16, 1.32	m	3.50	br. t (J = 6.0)
9	1.70	1.75, 1.55	m	1.94	m
10	0.97	0.81	t (J = 7.3)	0.98	t (J = 7.3)
11	4.06	3.92, 3.83	m	3.83	br. t (J = 5.9)
12–13	1.95, 1.70	2.00–1.40	m	2.00–1.40	m

	H$_2$L^4	Dinuclear [Ni$_2$(L^4)$_2$]		Mononuclear [NiL^4]	
	δ	δ	m (J, Hz)	δ	m (J, Hz)
4	6.90	6.52	br. d (J = 8.0)	6.62	dd (J = 7.7, J = 1.3)
5	6.75	6.29	dd (J = 8.0, J = 8.0)	6.39	dd (J = 7.7, J = 7.7)
6	6.85	6.25	dd (J = 8.0, J = 2.3)	6.71	br. d (J = 7.7)
7	8.30	6.29	br. s	7.85	br. s
8	3.55	4.25, 1.56	m	3.48	m
9	1.70	1.69	m	1.95	m
10	0.98	0.86	t (J = 7.7)	1.00	t (J = 7.3)
11	4.04	3.82	m	3.83	m
12	1.89	1.77	m	1.75	m
13	1.57	1.56	m	1.47	m

[a] Multiplicity, m, of the NMR signal.

(Table 4), to be compared to the value of 3.55 ppm found in the uncomplexed ligand. This kind of differentiation can be attributed to strong anisotropic effects generated by aromatic moieties. In particular, the methylene proton which gives the NMR signal at δ = 1.32 ppm should be in the full out-plane shielding cone generated by an aromatic ring which points at the proton, as expected for the helical arrangement of the dinuclear complex.

Moreover, an interesting trend was observed for the aromatic resonances: the H-6 proton was low-frequency shifted with respect to the H-4 proton (Table 4) and a remarkable low-frequency shift (δ = 1.81 ppm) was measured for the imine proton H-7. These data support a high shield for the imine proton and the adjacent aromatic proton (H-6) of the dinuclear species, according to their spatial proximity to the salicyl moiety of the second ligand, as expected on the basis of their helicate structure.

Confirmation of the nuclearity of the complex was obtained by measuring the diffusion coefficient of the freshly dissolved complex and comparing it with those of the free ligand and of a freshly dissolved sample of [Ni$_2$(L^8)$_2$] in CDCl$_3$ solution, which exists in a well defined dinuclear form.

The DOSY map of the [Ni$_2$(L^3)$_2$] complex (Figure 6, A) showed a single diffusion coefficient of 6.70×10^{-10} m^2 s^{-1}, lower than that of the H$_2$L^3 ligand ($D = 8.29 \times 10^{-10}$ m^2 s^{-1}), indicating an increase in the molecular sizes determined by the metal complexation, assigned to the dinuclear species on the basis of the X-ray (see previous paragraph).
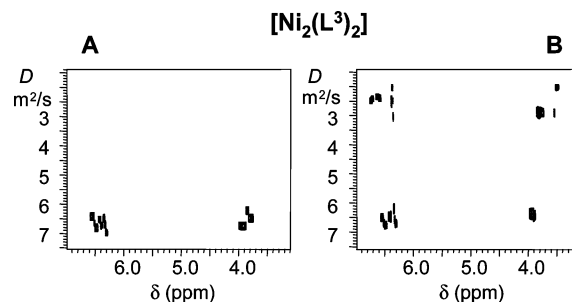

Figure 6. DOSY (600 MHz, CDCl$_3$, 25 °C) maps of [Ni$_2$(L^3)$_2$] freshly dissolved (A) and one week after dissolution (B).

A freshly dissolved sample of [Ni$_2$(L^8)$_2$] in CDCl$_3$ solution, prepared starting from crystals of the dinuclear species, showed both a unique set of resonances in the ^{1}H NMR spectrum and a single diffusion coefficient in the DOSY map ($D = 5.65 \times 10^{-10}$ m^2 s^{-1}), comparable to that of the [Ni$_2$(L^3)$_2$] complex.

It is noteworthy that no changes were detected either in the ^{1}H NMR spectrum or in the value of the diffusion coefficient of [Ni$_2$(L^8)$_2$] at different times. The diffusion coefficient of 5.65×10^{-10} m^2 s^{-1} can therefore be considered as evidence of a dinuclear species, apart from some deviations determined by the differences in the size of the ligands.

However, in solution the [Ni$_2$(L^3)$_2$] complex showed a behaviour quite different with respect to the [Ni$_2$(L^8)$_2$] one as it originated an interconversion equilibrium mixture

which, after one week, showed the presence of detectable amounts of the dinuclear complex (53%) and another species (47%), attributable to the mononuclear complex, as already evidenced in the case of the $[Ni_2(L^5)_2]\cdot THF$ complex.[3a]

The DOSY analysis of such an equilibrium mixture, which was fully characterized (Table 4), pointed out the presence of the dinuclear species ($D = 6.70 \times 10^{-10}$ m^{2}s^{-1}), already discussed, and for the mononuclear species an unexpectedly low diffusion coefficient ($D = 2.60 \times 10^{-10}$ m^{2}s^{-1}) was measured (Figure 6, B). As a matter of fact, the above value was too low not only for a mononuclear complex, but also for the dinuclear one and, hence, seemed to belong to a larger species.

With the aim of gaining a better insight into this aspect, we analysed, by DOSY technique, a solution of $[NiL^6]$, which exists as mononuclear complex.[3a] The measured diffusion coefficient for this species was 2.89×10^{-10} m^{2}s^{-1}, very similar to that measured in the equilibrium mixture obtained from the dissolution of the $[Ni_2(L^3)_2]$ complex.

Progressive dilution experiments of $[NiL^6]$ led to an approximately twofold concomitant increase in the diffusion coefficient ($D = 5.22 \times 10^{-10}$ m^{2}s^{-1} for a 1:20 dilution), supporting the self-association of the mononuclear species in solution. This behaviour is in accord with the well known phenomenon observed with Ni^{II} and Cu^{II} complexes of bidentate Schiff bases, which lead to the formation of dimers or polymers through intermolecular metal–oxygen interactions.[9]

The $[Ni_2(L^4)_2]$ complex behaved likewise to the already discussed $[Ni_2(L^3)_2]$ complex: in a freshly dissolved sample only one species with a diffusion coefficient of 6.50×10^{-10} m^{2}s^{-1} (Figure 7, A) was present, corresponding to a dinuclear species (see Table 4 for characterization). At equilibrium another species, with a diffusion coefficient of 1.70×10^{-10} m^{2}s^{-1}, was formed at the expense of the dinuclear species, attributable to the self-aggregated mononuclear complex (Figure 7, B). Accordingly, dilution measurements left the diffusion coefficient of the dinuclear complex unchanged, while bringing about a significant increment in the diffusion coefficient ($D = 4.00 \times 10^{-10}$ m^{2}s^{-1} for the 1:10 diluted solution) of the mononuclear complex formed by a disassembling process in solution.

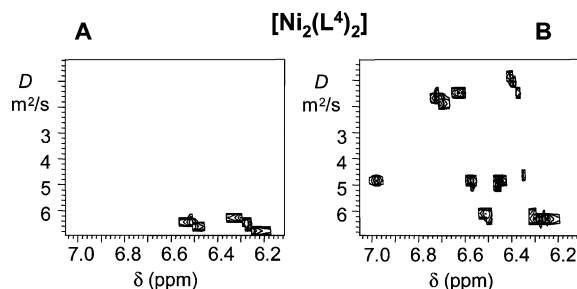Further evidence of the self-association of monomeric species came from ROE data. In fact, methyl protons (H-10) of the propyl chain produced ROEs on the bridging methylene chain (H-11, H-12 and H-13), which could not be attributed to intramolecular interactions and are in accordance with a stacking of monomeric units.

It is noteworthy that in this case a third species, characterized by an intermediate diffusion coefficient ($D = 4.90 \times 10^{-10}$ m^{2}s^{-1}) (Figure 7, B), which is unaffected by dilution, was detected. This value was quite similar to that observed for the dinuclear species. This last species could be a different conformation of the dinuclear complex, which is likely to be the face-to-face structure already discussed for $[Ni_2(L^1)_2]$. Accordingly, the methylene protons H-8 are isochronous as in the mononuclear species (Tables 5 and 6) and its H-7 protons are remarkably higher frequency shifted with respect to the same protons in the dinuclear helicate. As a matter of fact, in the double-stranded helical structure the H-7 protons and low-frequency shifted H-8 protons ($\delta = 1.56$ ppm) are faced to the aromatic rings, whereas for the face-to-face arrangement the H-7 and H-8 protons protrude from the coordination plane, far away from the aromatic rings and, hence, are unaffected by shielding anisotropic effects.

Table 5. ^{1}H NMR (600 MHz, CDCl$_3$, 25 °C) chemical shift (δ in ppm referenced to TMS as external standard) data of the third species observed in the equilibrium mixture originated by the $[Ni_2(L^4)_2]$ complex.

Proton	δ	$m^{[a]}$ (J, Hz)
4	6.58	d ($J = 7.8$)
5	6.45	dd ($J = 7.8$, $J = 7.8$)
6	6.71	d ($J = 7.8$)
7	6.98	s
8	3.08	t ($J = 6.5$)
9	1.82	m
10	0.97	t ($J = 7.4$)
11	3.83	m
12	1.74	m
13	1.46	m

[a] Multiplicity, m, of the NMR signal.

It should be noted that the conversion of the helicate to a face-to-face structure would be a low-energy process, as could occur through an intramolecular rearrangement involving an untwisting of the helicate structure without ligand dissociation. Thus, it is likely that the hexamethylene bridging unit provides optimal geometric requirements to gain access, through this pathway, to the face-to-face structure. On the other hand, similar topologies, not found in all the other cases studied, are not accessible for more rigid helicates. However, for helicates that contain longer and more flexible bridging units, such as octamethylene and dodecamethylene, similar face-to-face topologies may be accessible, although they are kinetically less stable.

Finally, for the $[Ni_2(L^1)_2]$ complex, for which ESI-MS analysis showed evidence of its nuclearity, DOSY analysis confirmed the presence of a species with a diffusion coefficient of 5.40×10^{-10} m^{2}s^{-1}, according to a dinuclear coordination complex.

Figure 7. DOSY (600 MHz, CDCl$_3$, 25 °C) maps of $[Ni_2(L^4)_2]$ freshly dissolved (A) and one week after dissolution (B).

Table 6. ^{1}H NMR (300 MHz, CDCl$_3$, 25 °C) chemical shift (δ, ppm referenced to TMS as external standard) of mononuclear ([NiL^5] and [NiL^6]) and dinuclear ([Ni$_2$(L^7)$_2$]·CHCl$_3$ and [Ni$_2$(L^8)$_2$]) complexes.

X	R	Ligand	Complex	δ				
				H-4	H-5	H-6	H-7	H-8
(CH$_2$)$_8$	nPr	H$_2$L^5	[NiL^5]	6.63	6.38	6.71	7.96	3.53
(CH$_2$)$_{12}$	nPr	H$_2$L^6	[NiL^6]	6.62	6.38	6.71	7.59	3.51
o-Xylidene	Me	H$_2$L^7	[Ni$_2$(L^7)$_2$]·CHCl$_3$	6.78	6.36	6.59	6.79	
o-Xylidene	nPr	H$_2$L^8	[Ni$_2$(L^8)$_2$]	6.72	6.34	6.57	6.63	3.81, 0.95

It is interesting to observe that dinuclear complexes have some common NMR spectroscopical features: they are all characterized by a remarkable anisochrony of the methylene protons of the propyl chains directly bound to the nitrogen atom (Tables 4 and 6); a reliable trend in the relative positions of the aromatic resonances is always found as the highest-frequency signal is originated from the H-4 protons (Tables 4 and 6); and, finally, the H-7 imine proton is low-frequency shifted with respect to the corresponding mononuclear species (Tables 4 and 6).

The contrary is true for the mononuclear complexes as they all have the H-6 protons resonating at higher frequency than the H-4 protons (Tables 4 and 6), with isochronous methylene protons H-8 giving rise to a signal at about 3.5 ppm, as observed in the free ligands.

In the case of [Ni$_2$(L^8)$_2$] (see Table 7 for characterization), where an *ortho*-xylidene bridging unit is present, the detection of intramolecular dipolar interactions originated by the methylene protons directly bound to the nitrogen atom allowed us to impose stereochemical constraints in solution which are in agreement with the double-stranded helicate structure determined by the X-ray analysis for the analogous [Ni$_2$(L^7)$_2$]·CHCl$_3$ complex.[3b]

Table 7. ^{1}H NMR (300 MHz, CDCl$_3$, 25 °C) chemical shift (δ in ppm referenced to TMS as external standard) data of the dinuclear Ni$_2$(L^8)$_2$ complex.

Proton	δ	m[a] (J, Hz)
4	6.72	d (J = 7.7)
5	6.34	dd (J = 7.7, J = 7.7)
6	6.57	d (J = 7.7)
7	6.63	s
8	3.81, 0.95	m
9	1.82, 1.50	m
10	0.77	t (J = 7.3)
11	5.12, 5.02	d (J = 13.4)
12	7.52	m
13	7.29	m

[a] Multiplicity, m, of the NMR signal.

Indeed, the high-frequency shifted proton H-8 (δ = 3.81 ppm) generated an intense NOE on the methylene protons H-11 of the *ortho*-xylidene bridge (Figure 8, a), whereas the low-frequency shifted methylene proton H-8 (δ = 0.95 ppm) produced an intense NOE on the imine proton H-7 (Figure 8, b) indicating an arrangement of the methyl-

ene group directly bound to the nitrogen atom, in which one proton is *cisoid* to the imine proton and the other proton, *transoid* to it, faces the *ortho*-xylidene bridge.
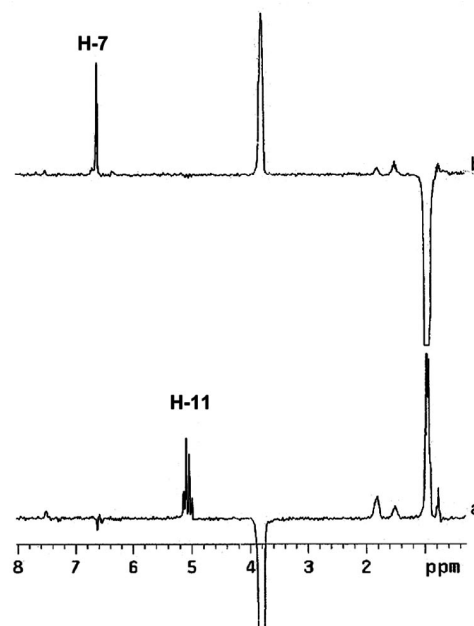

Figure 8. Traces of the ROESY map (300 MHz, CDCl$_3$, 25 °C, mix 0.4 s) of Ni$_2$(L^8)$_2$ corresponding to the high-frequency (a) and low-frequency (b) shifted resonances of methylene group H-8.

According to the X-ray structure,[3b] the proton of the methylene group bound to the nitrogen atom, in spatial proximity to the imine proton, is located in the shielding region of the salicyl moiety of the second ligand, whereas the proton of the same group, *transoid* to the imine proton, is far away from any aromatic shielding region and its chemical shift is similar to that measured for the corresponding isochronous methylene protons of the mononuclear species (Tables 4 and 7).

The length and flexibility of the bridging chains in the other complexes, together with the partial superimposition of some resonances, prevented us from obtaining stereochemical information in solution from NOE data.

Conclusions

In this paper we have described some new members of a class of ligands derived from two salicylaldiminato moieties,

connected at the 3-position by a α,ω-dioxo-polymethylene or α,α′-dioxo-*ortho*-xylidene bridge, and their coordination chemistry with Ni^{II} and Cu^{II}.

Taking into account the results of this work and those previously reported, it is possible to conclude that all these ligands are capable of generating, by self-assembly, interesting new compounds of varying nuclearity and unusual structural features.

The ligands $H_2L^{3–5,7,8}$, upon complexation to nickel(II) and – in the cases of H_2L^7 and H_2L^8 – to copper(II) ions, afford double-helical dinuclear complexes exhibiting as a special feature a *trans*-square-planar geometry around the metal ions.

With the ligands containing polymethylene spacers, the nuclearity of the complexes depends on the number of methylene units: by packing an increasing number of methylene groups in the linker chain, low nuclearity species are favoured. In fact, in the case of ligands with the tri- and tetramethylene spacers, oligomeric or polymeric materials are the final stable products of the reaction with the Ni^{II} and Cu^{II} ions. Accordingly, the dinuclear derivatives $[Ni_2(L^1)_2]$ and $[Cu_2(L^1)_2]$, to which face-to-face structures were attributed, are kinetic products which likely undergo a process of rearrangement to afford insoluble, thermodynamically stable species with higher nuclearities. On the other hand, the trend to higher nuclearities for the shorter ligands is not contradictory to the formation of the trinuclear circular helicate $[Ni_3(L^2)_3(py)_6]$ and of $[Ni_3(L^2)_2(OAc)_2]$, where the macrocyclic dinuclear structure encapsulates a molecule of nickel acetate. In fact, the first is the product of the competition of the strongly coordinating pyridine with the ligand $(L^2)^{2–}$, while in the case of the second one, which can only be achieved under high-dilution conditions, the stability of the cyclic dinuclear core can likely be ascribed to the encapsulation of the molecule of nickel acetate. When the number of linker chain atoms becomes 5, and up to 8, the ligands become binucleating and afford double-stranded nickel(II) helicates. However, while these complexes are stable in the solid state, a monomer–dimer interconversion process is observed in chloroform solution by NMR spectroscopy. In the equilibrium mixture the monomer to dimer ratio varies from the value 47/53, observed for the derivative with the pentamethylene spacer, to the value 95/5 of the derivative with the octamethylene spacer. These results indicate an increasing tendency of these ligands to become mononucleating as the length and the flexibility of the bridge increase. In accordance with this finding, we found[3a] the ligand H_2L^6, with the dodecamethylene bridge, to act only as a tetradentate chelating unit in the mononuclear complex $[NiL^6]$.

Furthermore, following these concepts, the polymethylene bridge was replaced by the short, rigid and helically preorganized *ortho*-xylidene unit to form the ligands H_2L^7 and H_2L^8. As expected, the dinuclearity and the helical structure of the related Ni^{II} and Cu^{II} complexes, found in the solid state, are maintained in chloroform solution, as determined on the basis of NMR and ESI-MS measurements.

Experimental Section

The ligand H_2L^2 was prepared as described previously.[3] IR spectra were collected on a Perkin–Elmer Paragon 500 FTIR spectrophotometer. ESI mass spectra were recorded with a PE Sciex API III plus triple quadrupole mass spectrometer equipped with an atmospheric pressure ionization source and an articulated ionspray interface. The sample was dissolved in chloroform (1 mg mL^{-1}) and diluted to 1:100 with acetonitrile. Experimental conditions included: IS voltage, 5.5 kV; OR voltage, 90 V. NMR measurements were performed on a Varian VXR-300 spectrometer operating at 300 MHz for ^{1}H and on a Varian INOVA 600 operating at 600 MHz for ^{1}H using a 5-mm broadband inverse probe with *z*-axis gradient. The sample temperature was maintained at 25 °C. The NMR spectra were recorded in $CDCl_3$ and the ^{1}H NMR chemical shifts were referenced to TMS as external standard. The 2D NMR spectra were obtained by using standard sequences. The double-quantum-filtered (DQF) COSY experiments were recorded with the minimum spectral width required; 256 increments of 8 scans and 2 K data points were acquired. The relaxation delay was 5 s. The data were zero-filled to 2 K × 1 K and a Gaussian function was applied for processing in both dimensions. The phase-sensitive ROESY spectra were acquired with the minimum spectral width required in 2 K data points using 8 scans for each of the 256 t_1 increments; the mixing time ranged from 200 to 600 ms. A Gaussian function was applied for processing in both dimensions. The gradient gHSQC spectrum was obtained in 32 transients per increment into a 2048 × 256-point data matrix and zero filled to 2048 × 1024 points. DOSY experiments were carried out by using a stimulated echo sequence with self-compensating gradient schemes, a spectral width of 8000 Hz and 32 K data points. Typically, a value ranging from 120 to 250 ms was used for Δ, 1.0 ms for δ, and *g* was varied in 30 steps (8 transients each) to obtain an approximately 90–95% decrease in the resonance intensity at the largest gradient amplitudes. The baselines of all arrayed spectra were corrected prior to processing the data. After data acquisition, each FID was apodized with 1.0-Hz line broadening and Fourier transformed. The data were processed with the DOSY macro (involving the determination of the resonance heights of all the signals above a pre-established threshold and the fitting of the decay curve for each resonance to a Gaussian function) to obtain pseudo-two-dimensional spectra with NMR chemical shifts along one axis and calculated diffusion coefficients along the other.

Preparation of Precursor Dialdehydes: These compounds were prepared from 2,3-dihydroxybenzaldehyde and relative dibromide according to our previously reported procedure.[3]

1,3-Bis(3-formyl-2-hydroxyphenoxy)propane: White crystals from cyclohexane, m.p. 112–120 °C. IR (Nujol): ṽ = 1658 (C=O) cm^{-1}. ^{1}H NMR ($CDCl_3$): δ = 11.05 (s, 2 H, OH), 9.87 (s, 2 H, CHO), 7.18–6.87 (m, 6 H, C_6H_3), 4.28 (t, 4 H, OCH_2), 2.37 (t, 2 H, CH_2) ppm. $C_{17}H_{16}O_6$ (316.09): calcd. C 64.55, H 5.10; found C 64.81, H 5.32.

1,5-Bis(3-formyl-2-hydroxyphenoxy)pentane: White crystals from chloroform/*n*-hexane, m.p. 102–106 °C. IR (Nujol): ṽ = 1652 (C=O) cm^{-1}. ^{1}H NMR ($CDCl_3$): δ = 11.05 (s, 2 H, OH), 9.93 (s, 2 H, CHO), 7.22–6.92 (m, 6 H, C_6H_3), 4.10 (t, 4 H, $ArOCH_2$), 2–1.7 [m, 6 H, $(CH_2)_3$] ppm. $C_{19}H_{20}O_6$ (344.12): calcd. C 66.27, H 5.85; found C 66.57, H 6.08.

1,6-Bis(3-formyl-2-hydroxyphenoxy)hexane: White crystals from chloroform/*n*-hexane, m.p. 138–142 °C. IR (Nujol): ṽ = 1652 (C=O) cm^{-1}. ^{1}H NMR ($CDCl_3$): δ = 11.07 (s, 2 H, OH), 9.93 (s, 2 H, CHO), 7.21–6.92 (m, 6 H, C_6H_3), 4.08 (t, 4 H, $ArOCH_2$), 1.92–

1.6 [m, 8 H, $(CH_2)_4$] ppm. $C_{20}H_{22}O_6$ (358.14): calcd. C 67.03, H 6.19; found C 66.92, H 6.28.

Preparation of the Ligands: The ligands were synthesized following standard procedures.[3]

H_2L^1: Yellow crystals from chloroform/*n*-hexane, m.p. 72–75 °C. IR (Nujol): $\tilde{v}$ = 1635 (C=N) cm^{-1}. ^{1}H NMR (CDCl$_3$): δ = 14.21 (s, OH), 8.29 (t, *J* = 1.2 Hz, 7-H), 6.97 (dd, *J* = 7.9, *J* = 1.6 Hz, 4-H), 6.85 (dd, *J* = 7.9, *J* = 1.6 Hz, 6-H), 6.74 (dd, *J* = 7.9, *J* = 7.9 Hz, 5-H), 4.29 (t, *J* = 6.1 Hz, 11-H), 3.55 (dt, *J* = 6.7, *J* = 1.2 Hz, 8-H), 2.41 (m, 12-H), 1.71 (m, 9-H), 0.98 (t, *J* = 7.5 Hz, 10-H) ppm. $C_{23}H_{30}N_2O_4$ (398.22): calcd. C 69.32, H 7.59, N 7.03; found C 69.54, H 7.22, N 6.86.

H_2L^3: Yellow crystals from chloroform/*n*-hexane, m.p. 40–43 °C. IR (Nujol): $\tilde{v}$ = 1632 (C=N) cm^{-1}. ^{1}H NMR (CDCl$_3$): δ = 14.19 (s, OH), 8.30 (t, *J* = 1.2 Hz, 7-H), 6.90 (dd, *J* = 8.0, *J* = 1.5 Hz, 4-H), 6.85 (dd, *J* = 7.8, *J* = 1.5 Hz, 6-H), 6.75 (dd, *J* = 8.0, *J* = 7.8 Hz, 5-H), 4.06 (t, *J* = 6.6 Hz, 11-H), 3.55 (dt, *J* = 6.6, *J* = 1.2 Hz, 8-H), 1.95 (m, 12-H), 1.70 (m, 9-H and 13-H), 0.97 (t, *J* = 7.5 Hz, 10-H) ppm. $C_{25}H_{34}N_2O_4$ (426.25): calcd. C 70.39, H 8.03, N 6.57; found C 70.52, H 8.15, N 6.29.

H_2L^4: Yellow crystals from chloroform/*n*-hexane, m.p. 100–103 °C. IR (Nujol): $\tilde{v}$ = 1632 (C=N) cm^{-1}. ^{1}H NMR (CDCl$_3$): δ = 14.19 (s, OH), 8.30 (t, *J* = 1.2 Hz, 7-H), 6.90 (dd, *J* = 8.0, *J* = 1.6 Hz, 4-H), 6.85 (dd, *J* = 7.8, *J* = 1.6 Hz, 6-H), 6.75 (dd, *J* = 8.0, *J* = 7.8 Hz, 5-H), 4.04 (t, *J* = 6.6 Hz, 11-H), 3.55 (dt, *J* = 6.8, *J* = 1.2 Hz, 8-H), 1.89 (m, 12-H), 1.70 (m, 9-H), 1.57 (m, 13-H), 0.98 (t, *J* = 7.4 Hz, 10-H) ppm. $C_{26}H_{36}N_2O_4$ (440.26): calcd. C 70.88, H 8.24, N 6.36; found C 70.66, H 8.01, N 6.18.

H_2L^8: Yellow crystals from chloroform/*n*-hexane, m.p. 74–79 °C. IR (Nujol): $\tilde{v}$ = 1630 (C=N) cm^{-1}. ^{1}H NMR (CDCl$_3$): δ = 14.18 (s, OH), 8.31 (t, *J* = 1.2 Hz, 7-H), 7.55 (m, 12-H), 7.31 (m, 13-H), 7.00 (dd, *J* = 8.0, *J* = 1.2 Hz, 4-H), 6.87 (dd, *J* = 7.8, *J* = 1.2 Hz, 6-H), 6.71 (dd, *J* = 8.0, *J* = 7.8 Hz, 5-H), 5.34 (s, 11-H), 3.56 (dt, *J* = 6.9, *J* = 1.2 Hz, 8-H), 1.73 (m, 9-H), 0.99 (t, *J* = 7.5 Hz, 10-H) ppm. $C_{28}H_{32}N_2O_4$ (460.23): calcd. C 73.02, H 7.00, N 6.08; found C 73.15, H 6.78, N 5.90.

Preparation of the Complexes: The complexes were synthesized following standard procedures.[3]

[Ni$_x$(L^1)$_x$]: Green microcrystalline powder, m.p. >240 °C. IR (Nujol): $\tilde{v}$ = 1614 (C=N) cm^{-1}. ESI-MS: *m/z* (%) = 399 (50) [H_2L^1 + H]$^+$, 455 (30) [NiL^1 + H]$^+$, 934 (2) [Ni$_2$(L^1)$_2$ + Na]$^+$. ^{1}H NMR (CDCl$_3$): δ = 7.97 (br. s, 7-H), 6.71 (br. d, *J* = 6.0 Hz, 6-H), 6.64 (br. d, *J* = 8.0 Hz, 4-H), 6.38 (dd, *J* = 6.0, *J* = 8.0 Hz, 5-H), 3.97 (m, 11-H), 3.51 (m, 8-H), 2.17 (m, 12-H), 1.93 (m, 9-H), 0.97 (t, *J* = 6.2 Hz, 10-H) ppm. $C_{23}H_{28}N_2NiO_4$: calcd. C 60.69, H 6.20, N 6.15; found C 60.77, H 6.36, N 6.02.

[Cu$_x$(L^1)$_x$]: Brown microcrystalline powder, m.p. >240 °C. IR (Nujol): $\tilde{v}$ = 1616 (C=N) cm^{-1}. ESI-MS: *m/z* (%) = 400 (80) [H_2L^1 + H]$^+$, 921 (10) [Cu$_2$(L^1)$_2$ + H]$^+$, 944 (15) [Cu$_2$(L^1)$_2$ + Na]$^+$. $C_{23}H_{28}CuN_2O_4$ (460.03): calcd. C 60.05, H 6.13, N 6.09; found C 60.13, H 6.22, N 6.28.

[Ni$_2$L$^3_2$]·*n*-heptane: Green crystals from chloroform/*n*-heptane, m.p. 125–126 °C. IR (Nujol): $\tilde{v}$ = 1610 (C=N) cm^{-1}. ESI-MS: *m/z* (%) = 427 (100) [H_2L^1 + H]$^+$, 483 (83) [NiL^1 + H]$^+$, 910 (8) [Ni(L^1)$_2$ + 3 H]$^+$, 965 (10) [Ni$_2$(L^1)$_2$ + H]$^+$. ^{1}H NMR, see text. $C_{57}H_{80}N_4Ni_2O_8$ (1064.47): calcd. C 64.18, H 7.56, N 5.25; found C 64.36, H 7.73, N 5.27.

[(Ni)$_2$(L^4)$_2$]: Green microcrystalline powder from chloroform/*n*-heptane, m.p. 132–134 °C. IR (Nujol): $\tilde{v}$ = 1610 (C=N) cm^{-1}. ESI-MS: *m/z* (%) = 441 (80) [H_2L^1 + H]$^+$, 497 (100) [NiL^1 + H]$^+$, 938 (5) [Ni(L^1)$_2$ + 3 H]$^+$, 965 (traces) [Ni$_2$(L^1)$_2$ + H]$^+$. ^{1}H NMR, see text. $C_{52}H_{68}N_4Ni_2O_8$ (992.37): calcd. C 62.80, H 6.89, N 5.63; found C 62.97, H 6.94, N 5.82.

[(Ni)$_2$(L^8)$_2$]: Green microcrystalline powder from chloroform/*n*-heptane, m.p. 194–199 °C. IR (Nujol): $\tilde{v}$ = 1616 (C=N) cm^{-1}. ESI-MS: *m/z* (%) = 461 (70) [H_2L^7 + H]$^+$, 517 (38) [NiL^7 + H]$^+$, 977 (5) [Ni(L^7)$_2$ + 3 H]$^+$, 1033 (traces) [Ni$_2$(L^7)$_2$ + H]$^+$. ^{1}H NMR, see text. $C_{56}H_{60}N_4Ni_2O_8$ (1032.31): calcd. C 65.02, H 5.85, N 5.42; found C 65.18, H 5.91, N 5.36.

[(Cu)$_2$(L^8)$_2$]: Brown crystals from chloroform/*n*-heptane, m.p. 168–172 °C. IR (Nujol): $\tilde{v}$ = 1620 (C=N) cm^{-1}. ESI-MS: *m/z* (%) = 461 (100) [H_2L^8 + H]$^+$, 1046 (10) [Cu$_2$(L^8)$_2$ + H]$^+$, 1067 (25) [Cu$_2$(L^8)$_2$ + Na]$^+$. $C_{56}H_{60}Cu_2N_4O_8$ (1044.22): calcd. C 64.41, H 5.79, N 5.37; found C 64.67, H 5.95, N 5.58.

Preparation of [Ni$_3$(L^2)$_2$·(OAc)$_2$]·CH$_3$CN: A solution of Ni(OAc)$_2$·4H$_2$O (0.24 g, 0.97 mmol) in MeOH (100 mL) was added dropwise to a solution of H_2L^2 (0.4 g, 0.97 mmol) in MeOH (600 mL). The solution obtained was concentrated (10 mL), added to H$_2$O (50 mL) and extracted with chloroform (3 × 50 mL). The combined organic layers were dried with Na$_2$SO$_4$, concentrated and added to Et$_2$O (20 mL). The solid precipitated was collected by filtration, washed with diethyl ether and dried in vacuo (0.28 g). Recrystallization from acetonitrile led to green crystals, m.p. > 240 °C. IR (Nujol): $\tilde{v}$ = 1626 (COO$^-$), 1614 (C=N) cm^{-1}. ESI-MS: *m/z* (%) = 414 (20) [H_2L^2 + H]$^+$, 469 (50) [NiL^2 + H]$^+$, 1044 (5) [Ni$_2$(L^2)$_2$·OAc + Na$_2$]$^+$, 1133 (10) [Ni$_3$(L^2)$_2$·(OAc)$_2$ + Na]$^+$. $C_{52}H_{66}N_4Ni_3O_{12}$·CH$_3$CN (1153.30): calcd. C 56.09, H 6.02, N 6.06; found: C 56.19, H 6.26, N 6.16.

X-ray Diffraction Studies: The X-ray diffraction experiments were carried out at room temperature (T = 293 K) by means of a Bruker P4 four-circle diffractometer. In all experiments graphite-monochromated Mo-K_α radiation was used. The samples were glued at the top of glass fibres and handled in air. The intensities were corrected for Lorentz and polarization effects and for absorption by the ψ-scan method[10] for [Ni$_3$(L^2)$_2$(OAc)$_2$]·acetonitrile and [Cu$_2$(L^8)$_2$] and by an integration method based on the crystal habit[11] for [Ni$_2$(L^3)$_2$]·*n*-heptane. The structure solutions were obtained by means of the automatic direct methods contained in the SHELXS97 program[12] for [Ni$_3$(L^2)$_2$(OAc)$_2$]·acetonitrile and [Ni$_2$(L^3)$_2$]·*n*-heptane and in the SIR-92 program[13] for [Cu$_2$(L^8)$_2$]. The refinement, based on full-matrix least-squares on F^2, were done by means of the SHELXL97[12] program. Some other utilities contained in the WINGX suite[14] were also used. The more relevant crystal parameters are listed in Table 8.

The structure solution of [Ni$_3$(L^2)$_2$(OAc)$_2$]·acetonitrile was found in the $P\bar{1}$ space group. The difference Fourier map showed the presence of a lattice acetonitrile molecule. One of the ligands presented disorder in one of the terminal propyl groups and in the intermediate C$_4$ chain. Both of the disordered groups were refined as distributed in two different positions. The hydrogen atoms were placed in calculated positions and left to ride on the connected carbon atoms. The final refinement cycles were performed with anisotropic thermal parameters for heavy atoms that were not disordered and isotropic for the others, giving the final reliability factors listed in Table 8.

[Ni$_2$(L^3)$_2$]·*n*-heptane crystallizes in the trigonal symmetry class and the structure solution was found in the chiral space group $P3_121$. The asymmetric unit is made up of one half molecule placed near the Wickoff position *a* astride a twofold axis which generates the whole molecule. The packing of the molecules leaves a channel along the threefold screw-helix 3_1, where a series of electron density

Table 8. Crystal data and structure refinements.

Compound	[Ni$_3$(L^2)$_2$(OAc)$_2$]·acetonitrile	[Ni$_2$(L^3)$_2$]·n-heptane	[Cu$_2$(L^8)$_2$]
Empirical formula	C$_{54}$H$_{69}$N$_5$Ni$_3$O$_{12}$	C$_{57}$H$_{80}$N$_4$Ni$_2$O$_8$	C$_{56}$H$_{60}$Cu$_2$N$_4$O$_8$
Formula weight	1156.27	1066.67	1044.16
Crystal system	triclinic	trigonal	monoclinic
Space group	$P\bar{1}$ (no. 2)	$P3_121$ (no. 152)	$C2/c$ (no. 15)
a [Å]	13.313(2)	18.964(3)	21.516(3)
b [Å]	13.648(2)	18.964(3)	9.002(1)
c [Å]	16.390(3)	13.013(4)	27.510(3)
α [°]	93.43(1)	90	90
β [°]	100.64(1)	90	107.652(7)
γ [°]	110.186(7)	120	90
U [Å^3]	2722.4(6)	4053.0(15)	5077.3(11)
Z	2	3	4
D_{calcd} [Mg m^{-3}]	1.411	1.311	1.366
μ [mm^{-1}]	1.092	0.754	0.897
No. of measured reflections	8233	4589	3821
No. of unique reflections [R_{int}]	7131 [0.0171]	3423 [0.0525]	2986 [0.0472]
No. of parameters	670	296	317
R_1, wR_2 [$I > 2\sigma(I)$][a]	0.0386, 0.0878	0.0636, 0.1246	0.0674, 0.1174
R_1, wR_2 [all data][a]	0.0573, 0.0971	0.1493, 0.1578	0.1692, 0.1547
Goodness of fit[a] on F^2	1.001	1.003	1.045

[a] $R(F_o) = \Sigma||F_o| - |F_c||/\Sigma|F_o|$; $Rw(F_o^2) = \{\Sigma[w(F_o^2 - F_c^2)^2]/\Sigma[w(F_o^2)^2]\}1/2$; $w = 1/[\sigma^2(F_o^2) + (AQ)^2 + BQ]$ where $Q = [MAX(F_o^2, 0) + 2F_c^2]/3$; GOF $= [\Sigma[w(F_o^2 - F_c^2)^2]/(N - P)]1/2$, where N and P are the number of observations and parameters, respectively.

maxima were attributed to a disordered lattice n-heptane molecule. The disorder present in this site of the structure induced disorder in two propyl moieties of the [Ni$_2$(L^3)$_2$] molecule. The disordered propyl group was refined as distributed in two different conformations, by fixing to one the total occupancy for each atom. For the disordered solvent molecule, it was impossible to recognize any conformation and the maxima positions were introduced in the model as carbon atoms and left free to move in the refinement process. The hydrogen atoms of the [Ni$_2$(L^3)$_2$] molecule were introduced in calculated positions and left to move riding on the connected carbon atoms. The hydrogen atoms of the disordered solvent were disregarded. The final refinement cycles were performed with anisotropic thermal parameters for all the ordered heavy atoms and isotropic for the others. The final reliability factors are listed in Table 8.

The structure solution of [Cu$_2$(L^8)$_2$] was found in the $C2/c$ space group. The molecule, which possesses a twofold axis, is placed on the Wickoff position e and the copper atoms lie on the axis. The asymmetric unit consists of one half molecule. The hydrogen atoms were placed in calculated positions and left to ride on the connected carbon atoms during the refinement. The final refinement cycles were performed with anisotropic thermal parameters for all heavy atoms. The markedly prolated thermal ellipsoids of the atoms around Cu(1) suggest the presence of some degree of disorder in this part of the molecule. We have, however, disregarded the possibility of refining these atoms as distributed in different positions, leaving the electron density spreading to be described by thermal parameters alone. The final reliability factors are listed in Table 8.

CCDC-663354 (for [Ni$_3$(L^2)$_2$·(OAc)$_2$]·acetonitrile), -663355 (for [Ni$_2$(L^3)$_2$]·n-heptane) and -663356 (for [Cu$_2$(L^8)$_2$]) contain the supplementary crystallographic data for this paper. These data can be obtained free of charge from The Cambridge Crystallographic Data Centre via www.ccdc.cam.ac.uk/data_request/cif.

Supporting Information (see also the footnote on the first page of this article): ORTEP and space-filling representations of [Ni$_3$(L^2)$_3$(py)$_6$] and ball-and-stick representations of [Ni$_2$(L^3)$_2$] and [Cu$_2$(L^8)$_2$].

[1] a) M. Albrecht, I. Janser, H. Houjou, R. Fröhlich, *Chem. Eur. J.* **2004**, *10*, 2839–2850; b) F. Tuna, M. R. Lees, G. J. Clarkson, M. J. Hannon, *Chem. Eur. J.* **2004**, *10*, 5737–5750; c) P. J. Steel, *Acc. Chem. Res.* **2005**, *38*, 243–250; d) M. Vázquez, M. R. Bermejo, M. Licchelli, A. M. González-Noya, R. M. Pedrido, C. Sangregorio, L. Sorace, A. M. García-Deibe, J. Sanmartín, *Eur. J. Inorg. Chem.* **2005**, 3479–3490.

[2] a) Y. Song, I. A. Koval, P. Gamez, G. A. van Albada, I. Mutikainen, U. Turpeinen, J. Reedijk, *Polyhedron* **2004**, *23*, 1769–1775; b) A. M. García-Deibe, J. Sanmartın Matalobos, M. Fondo, M. Vazquez, M. R. Bermejo, *Inorg. Chim. Acta* **2004**, *357*, 2561–2569; c) Y. B. Xie, C. Zhang, J. R. Li, X. H. Bu, *Dalton Trans.* **2004**, 562–569; d) T. K. Ronson, H. Adams, M. D. Ward, *Inorg. Chim. Acta* **2005**, *358*, 1943–1954, and references cited therein; e) S. P. Argent, H. Adams, T. Riis-Johannessen, J. C. Jeffery, L. P. Harding, W. Clegg, R. W. Harrington, M. D. Ward, *Dalton Trans.* **2006**, 4996–5013; f) T. K. Ronson, H. Adams, T. Riis-Johannessen, J. C. Jeffery, M. D. Ward, *New J. Chem.* **2006**, *30*, 26–28; g) R. M. Yeh, K. N. Raymond, *Inorg. Chem.* **2006**, *45*, 1130–1139.

[3] a) L. Carbonaro, M. Isola, V. Liuzzo, F. Marchetti, F. Balzano, C. S. Pomelli, A. Raffaelli, *Eur. J. Inorg. Chem.* **2001**, 353–357; b) M. Isola, V. Liuzzo, F. Marchetti, A. Raffaelli, *Eur. J. Inorg. Chem.* **2002**, 1588–1590.

[4] V. Kessar, Y. P. Gupta, T. Mohammed, K. Sawal, *J. Chem. Soc. Chem. Commun.* **1983**, 400–401.

[5] a) M. Albrecht, *Chem. Rev.* **2001**, *101*, 3457–3497; b) S. Sailaja, M. V. Rajasekharan, *Inorg. Chem.* **2003**, *42*, 5675–5684; c) L. J. Childs, M. Pascu, A. J. Clarke, N. W. Alcock, M. J. Hannon, *Chem. Eur. J.* **2004**, *10*, 4291–4300; d) S. T. Onions, S. L. Heath, D. J. Price, R. W. Harrington, W. Clegg, C. J. Matthews, *Angew.*

Chem. Int. Ed. **2004**, *43*, 1814–1817; e) J. M. Senegas, S. Koeller, G. Bernardinelli, C. Piguet, *Chem. Commun.* **2005**, 2235–2237; f) S. P. Argent, H. Adams, T. Riis-Johannessen, J. C. Jeffery, L. P. Harding, O. Mamula, M. D. Ward, *Inorg. Chem.* **2006**, *45*, 3905–3919.

[6] a) B. J. McNelis, L. C. Nathan, C. J. Clark, *J. Chem. Soc. Dalton Trans.* **1999**, 1831–1834; b) G. F. Swiegers, J. Malefetse, *Coord. Chem. Rev.* **2002**, *225*, 91–121; c) C. Piguet, M. Borkovec, J. Hamacek, K. Zeckert, *Coord. Chem. Rev.* **2005**, *249*, 705–726.

[7] a) B. Hasenknopf, J.-M. Lehn, N. Boumediene, E. Leize, A. Van Dorsselaer, *Angew. Chem. Int. Ed.* **1998**, *37*, 3265–3268; b) M. Scherer, D. L. Caulder, D. W. Johnson, K. N. Raymond, *Angew. Chem. Int. Ed.* **1999**, *38*, 1588–1592; c) V. Berl, I. Huc, R. G. Khoury, J.-M. Lehn, *Chem. Eur. J.* **2001**, *7*, 2810–2820; d) Y. Sunatsuki, Y. Motoda, N. Matsumoto, *Coord. Chem. Rev.* **2002**, *226*, 199–209; e) T. Yano, R. Tanaka, T. Nishioka, I. Kinoshita, K. Isobe, L. J. Wright, T. J. Collins, *Chem. Commun.* **2002**, 1396–1397; f) M. Du, X.-H. Bu, Y.-M. Guo, J. Ribas, C. Diaz, *Chem. Commun.* **2002**, 2550–2551; g) M. Barboiu, G. Vaughan, N. Kyritsakas, J.-M. Lehn, *Chem. Eur. J.* **2003**, *9*, 763–769; h) V. Amendola, L. Fabbrizzi, P. Pallavicini, E. Sartirana, A. Taglietti, *Inorg. Chem.* **2003**, *42*, 1632–1636; i) J.-M. Senegas, S. Koeller, G. Bernardinelli, C. Piguet, *Chem. Commun.* **2005**, 2235–2237 and references cited therein; j) G. Bokolinis, T. Riis-Johannessen, L. P. Harding, J. C. Jeffery, N. McLaya, C. R. Rice, *Chem. Commun.* **2006**, 1980–1982.

[8] a) C. S. Johnson Jr, *Prog. Nucl. Magn. Reson. Spectrosc.* **1999**, *34*, 203–256; b) *Magn. Reson. Chem.* **2002**, *40*, Special Issue, NMR and Diffusion, S1–S152.

[9] a) D. Hall, T. N. Waters, *J. Chem. Soc.* **1960**, 2644–2648; b) J. Ferguson, *Spectrochim. Acta* **1961**, *17*, 316–323; c) D. Hall, S. V. Sheat, T. N. Waters, *J. Chem. Soc. Chem. Commun.* **1966**, 436–437; d) R. Klement, F. Stock, H. Elias, H. Paulus, P. Pelikan, M. Valko, M. Mazur, *Polyhedron* **1999**, *18*, 3617–3628.

[10] G. M. Sheldrick, *SHELXTL-Plus*, rel. 5.1, Bruker AXS Inc., Madison, WI, USA, **1997**.

[11] A. L. Spek, *PLATON, A Multipurpose Crystallographic Tool*, Utrecht University, Utrecht, The Netherlands, **1998**.

[12] G. M. Sheldrick, *SHELX97, Programs for Crystal Structure Analysis* (rel. 97-2), University of Göttingen, Göttingen, Germany, **1998**.

[13] A. Altomare, G. Cascarano, C. Giacovazzo, A. Guagliardi, *J. Appl. Crystallogr.* **1993**, *26*, 343–350.

[14] L. J. Farrugia, *J. Appl. Crystallogr.* **1999**, *32*, 837–838.